PREDICTION AND INVESTIGATION OF SURFACE ROUGHNESS WHILE TURNING SG IRON WITH CUBIC BORON NITRIDE (CBN) AND TUNGSTEN CARBIDE INSERTS

K.M. Kumar[1,2] and P. Hariharan[2]
[1]*St. Joseph's College of Engineering, Sholinganallur, Chennai, Tamilnadu, India*
[2]*College of Engineering, Anna University, Chennai, Tamilnadu, India*
E-mail: kumarkm@stjosephs.ac.in

Received May 2016, Accepted August 2016
No. 16-CSME-79, E.I.C. Accession 3965

ABSTRACT

This work compares the effect of cubic boron nitride (CBN) and multilayer (TiCN+Al_2O_3+TiN) coated tungsten carbide (WC) tools during the turning of spheroidal graphite (SG) nodular iron. Nodular irons have more ductility which is required in mechanical components that demand high fatigue resistance like crankshafts, cam shafts, bearing caps and clutch housings. The impact of various process parameters like the depth of cut, cutting speed and feed on the surface roughness (R_a) of SG iron is studied and optimized using the response surface model. The chip morphology is also discussed for evaluation of the quality of the turned surface. The experimental outcomes reveal that the WC tool offers a high surface finish at the optimal combination of the cutting speed at 102 meter/minute, feed at 0.051 millimeter/revolution and depth of cut at 0.5 millimeter and that, for the CBN insert, at 245 meter/minute of cutting speed, 0.051 millimeter/revolution of feed and 0.75 millimeter of depth of cut.

Keywords: roughness, machining, RSM, morphology, CBN, multilayer, ductile iron.

PRÉDICTION ET INVESTIGATION DE LA RUGOSITÉ DE LA SURFACE PENDANT LE TOURNAGE DE FONTE SG AVEC NITRURE DE BORE CUBIQUE ET INSERTION DE CARBURE DE TUNGSTÈNE

RÉSUMÉ

Le travail de recherche présent porte sur un procédé de conception innovateur d'un moteur électrique rotatif à mécanisme d'engrenage et aimant permanent intégré. Un moteur courant continu à commutation et un système mécanique à engrenage planétaire sont utilisés comme exemple. En se basant sur les exigences et contraintes de conception, un concept détaillé du rotor et du stator est obtenu. Une méthode de circuit magnétique équivalent à 1-D est appliquée pour analyser la performance du dispositif intégré, et il est vérifié par le logiciel FEM. Les méthodes de conception pour les trains d'engrenage, les profils, le nombre de dents, et la puissance de l'engrenage sont aussi introduites. Finalement nous obtenons un dispositif intégré réalisable qui réduit le couple d'encochage et l'ondulation du couple de 92.02% et de 50.14% respectivement, tandis que la densité de couple est augmentée de 16.66%.

Mots-clés : moteur électrique rotatif à mécanisme d'engrenage et aimant intégré; conception du moteur; procédé de conception intégré; mécanisme d'engrenage.

1. INTRODUCTION

Ductile irons like nodular ductile iron/spheroidal graphite (SG) iron, compacted graphite iron and tempered ductile iron are currently used in automotive, energy, wind power industries and construction of machines [1, 2]. Nodular iron is utilized as a part of wheels, crankshafts, and camshafts. Added substances including, for example, molybdenum (Mb), magnesium (Mg), copper (Cu), silicon (Si) and chromium (Cr) can be used for enhancing the mechanical properties of SG cast iron. But the addition of these additives results in poor machinability for SG iron [3]. The percentages of machinability are comparable to high strength steel alloys, like AISI 1110 steel and AISI 4140 steels [4]. The SG iron structure with graphite content is represented as tiny round spheroidal shapes in its matrix [5]. A small quantity of Mg, when injected into ductile iron, exists in round shapes that give prevalent flexibility and high quality and durability. Increasing either hardness or ductility reduces machinability. The most exciting challenges to metallurgists are to elevate the quality of materials with a minimum increase in cost, which has been accomplished by alloying, cold working, utilization of phase alterations, and the modification of grain dimension and microstructure. Accordingly, the need for machining has turned out to be more upon material microstructures.

Ductile iron is effortless to machine. However, it generates BUE on the tool due to its higher ferrite content. Certain grates of SG iron machining result in quick wear due to pearlite substance. During the machining of ductile cast iron, the graphite particles decide the cutting forces and surface irregularities [5, 6]. For machining SG iron, it is useful to get some reasonable cutting parameter values from the machining handbook [7–9]. The machinability of ductile cast irons depends on their microstructure, alloy content, hardness, and ductility.

Nowadays, different types of coated carbide tools are used for machining hardened materials like SG iron, austempered ductile iron, high strength steel alloys etc., The main coating materials like TiC, Al2O3, TiN and TiCN coatings improve the cutting tool wear resistance and maintain the toughness of cemented carbide [10, 11]. Most of the multilayer CVD coated carbide tools like TiCN+Al2O3+TiN are used for machining austempered ductile iron [12, 13]. SiN tools perform poorly when used for machining ductile iron. Coated tools show superior performance. Tungsten carbide substrates with a coating of TiCN/Al2O3/TiN are used in the early period for machining SG iron. The coating of TiCN diminishes and the impact of the Al2O3 becomes overwhelming at higher speeds. It is evident that the use of the latest multi-layered carbide tool decreases the flank wear by 40% at 200 meter/minute speeds in comparison with conservative coated carbide. Also, the latest grades likewise accomplish a 25% enhancement in tool life at 300 meter/minute [14].

Either a ceramic/CBN tool or a coated tool is used for dry machining to face the extraordinary heat produced by the operation. Low thermal conductivity and low friction coefficient coatings are excellent at separating a tool from heat. TiAlN coatings are greatly suggested for dry machining of cast ferrous materials, including cast irons [14].

The primary purpose of this experimental study is to compare the cutting operation of the two different cutting tools (CBN and coated WC tools) in view of workpiece R_a and chip morphology of ductile iron. The results observed on the R_a of SG iron with CBN and coated WC tools are reported, along with the examination results of chip morphology. A limited literature survey has been reported in ductile iron machining with CBN and coated WC tools. Since there is an absence of any related work carried out on the machining of ductile iron with CBN tool, an effort has been made to determine the optimum machining parameters.

2. MATERIALS AND METHODS

2.1. Materials, Experimental Set-up and Measurement

The material used in the turning experiments was a ductile cast iron (SG iron). The work material composition is shown in Table 1. The work materials were mixed with additives like molybdenum (Mb) and Nickel (Ni) for enhancing the mechanical properties of the SG iron apart from the ordinary chemical composition

Table 1. Chemical composition (wt%).

C	Si	Mn	P	S	Mo	Mg	Ni	Cu
3.65	2.8	0.32	0.031	0.012	0.2	0.035	1.29	0.53

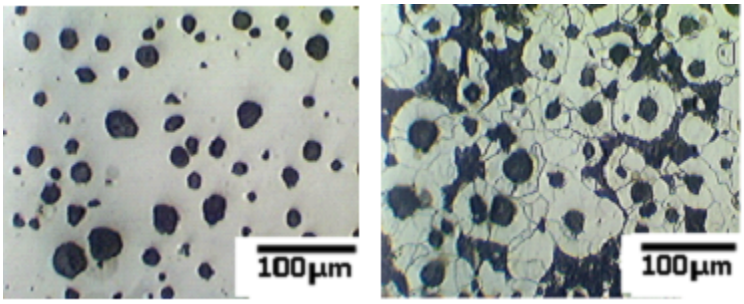

Fig. 1. Material microstructure.

of the ductile iron. The material microstructure is presented in Fig. 1. The etched microstructures show the nodular graphite enclosed by a matrix of ferrite and pearlite. The average diameter of the nodules is 20–50 µ and the number of nodules is 190 counts per mm^2. The percentage of ferrite is 62% and of pearlite is 38%. For turning experiments, the work specimen was cast as a hollow round bar with uniform cross sections of an external diameter of 65 millimeter and an inner diameter of 30 millimeter with a length of 300 millimeter. To assure the smooth surface, the work materials were machined with 0.5 millimeter of depth of cut before machining.

The experimental works were conducted on a conventional high speed lathe. The experimental setup with actual machining is illustrated in Fig. 2. In the present study, a CBN (CNMN120408) and coated WC Tool (CNMG 120408) were used as cutting tools. The cutting inserts were mounted on a tool holder PCLNL 2020 K12.

After completing each experiment, the workpiece surface roughness (R_a) was measured using a SURFTEST SJ-201P surface measuring instrument. The R_a was assessed by utilizing the 0.8 millimeter cut off length and a 4 millimeter evaluation length. The outcomes were taken and recorded in three areas close to the perimeter of the workpieces and repeated thrice at every point. Chip characteristics, obtained from all the experiments were observed using the video measuring system (VMC 2010) of opus make.

2.2. Experimental Design

The response surface methodology (RSM) is an accumulation of numerical and statistical measures, utilized for the analysis of quandaries in which the desired output is influenced by numerous parameters [15]. The RSM tool was employed for planning the experiments with selected cutting conditions. The analysis aims to use RSM with different cutting states using the Design-Expert (version 7) software. The levels and the process parameter for this investigation are given in Table 2. The experiments were conducted in three process parameters with three levels each consisting of 20 experimental runs (Table 3) in which every tool takes a central composite face-centered factorial design into account.

3. RESULTS AND DISCUSSIONS

3.1. Surface Roughness of SG Irons with CBN Tool

The most vital parameter for selecting the cutting inserts is the surface quality [3]. The cutting parameters and tool wear are the additional impacting parameters on the surface finish. A higher degree of surface finish was obtained with ceramic tools, which contrasts the results obtained from machining with traditional tools

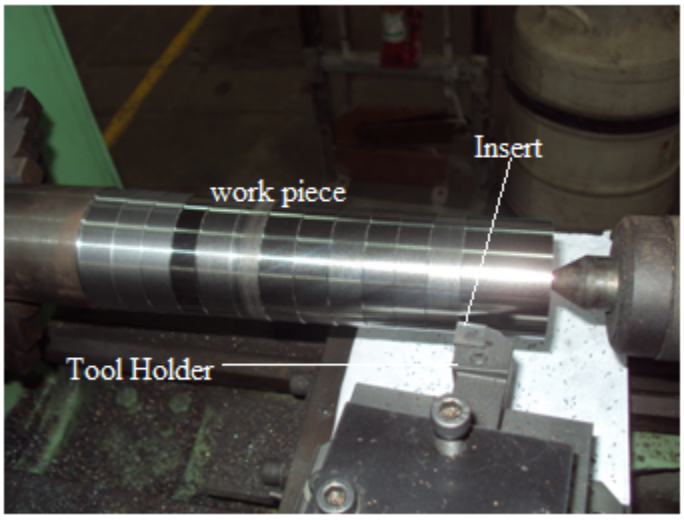

Fig. 2. Experimental set-up.

Table 2. Process parameter and their levels.

	Levels of factors		
Parameters	Level 1	Level 2	Level 3
Cutting speed (v) (m/min)	102	174	245
Feed (f) (mm/rev)	0.051	0.102	0.143
Depth of cut (d) (mm)	0.5	0.75	1

like cemented carbides [3]. The insert radius, feed, and depth of cut are associated with R_a of the materials [10].

The inputs for the expectation model utilizing RSM with machining parameters like feed, depth of cut, cutting speed and R_a have been taken as a response. Figure 5 shows the response quality characteristics, after machining with CBN tool under optimal machining conditions.

Using the least square fitting model, the following second order equation for R_a with cutting parameters has been developed.

$$R_a = +3.47957 + 0.067919 * v + 71.27597 * f - 27.49582 * d - 1.95187E - 004 * s^2 - 374.85374 * f^2 + 18.21455 * d^2 \quad (1)$$

Analysis of variance (ANOVA) techniques based on F and P-values were utilized for verifying the adequacy of the model. The F-value of the model 26.19 in ANOVA Table 4 indicates the significance of the model. There is only a 0.01% chance that a "Model F-value" this large could occur due to noise. The values of "prop $> F$" less than 0.05 indicates the model terms are significant. In this model, v^2, f^2, and d^2 are an important model term. The desired model does not consider the lack of fit as significant. The R^2 value which is 0.9236 is close to unity and the model is very efficient.

ANOVA demonstrates the existence of a high relationship between investigations and predicted value since the "Adjusted R^2" value (0.8883) is in practical concurrence with the "Predicted R^2" value (0.7849). The non-inclusion of irrelevant terms in this example is shown. Signal to noise ratio has been measured by "Adeq Precision". The ratio, which is larger than four, is normally attractive. The proportion of 17.565 establishes a satisfactory signal for this situation. Lower estimation of the coefficient of variation (C.V. = 10.10%) demonstrates enhanced exactness and reliability of the experimental trials.

Table 3. Experimental design with original values.

Run	Process Parameters		
	Cutting speed (v) (m/min)	Feed (f) (mm/rev)	Depth of cut (d) (mm)
1	102	0.143	1
2	245	0.143	0.5
3	174	0.102	0.5
4	102	0.143	0.5
5	174	0.102	0.75
6	174	0.102	1
7	174	0.102	0.75
8	245	0.102	0.75
9	245	0.051	0.5
10	102	0.051	0.5
11	174	0.143	0.75
12	102	0.051	1
13	174	0.051	0.75
14	245	0.051	1
15	245	0.143	1
16	174	0.102	0.75
17	102	0.102	0.75
18	174	0.102	0.75
19	174	0.102	0.75
20	174	0.102	0.75

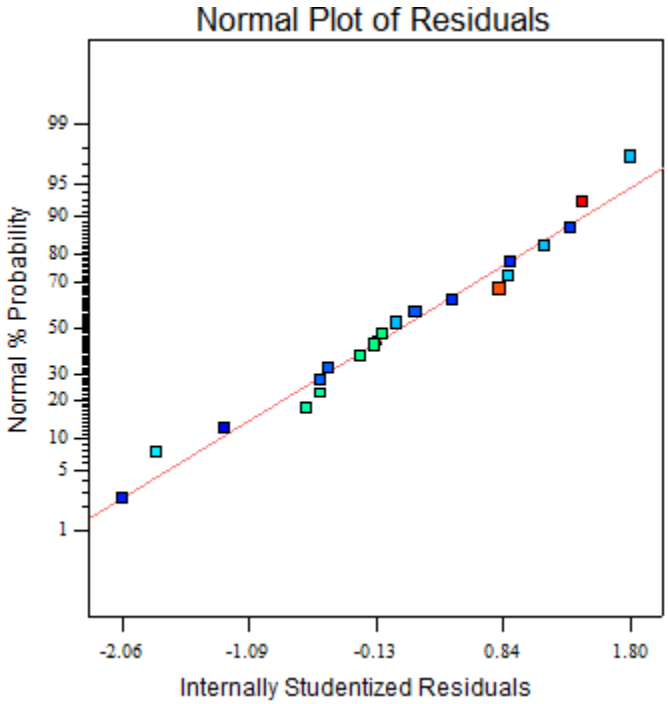

Fig. 3. Normal probability plot of residuals for surface roughness.

The diagnostics details of this model have been carried out by using residuals versus results. These are presented in Figs. 3 to 5. The normal plot of residuals (Fig. 3) shows the residuals being very near to a

Table 4. ANOVA results for surface roughness in turning SG iron with CBN insert.

Source	Sum of Squares	df	Mean Square	F Value	p-value Prob $> F$	Remarks
Model	6.64	6	1.11	26.19	< 0.0001	Significant
v-cutting speed	1.823E-03	1	1.823E-03	0.043	0.8388	
f-feed	0.044	1	0.044	1.05	0.3252	
d-depth of cut	0.019	1	0.019	0.45	0.5153	
v^2	2.42	1	2.42	57.20	< 0.0001	
f^2	1.68	1	1.68	39.82	< 0.0001	
d^2	3.56	1	3.56	84.27	< 0.0001	
Residual	0.55	13	0.042			
Lack of fit	0.47	8	0.059	3.90	0.0752	Not significant
Pure error	0.076	5	0.015			
Cor Total	7.19	19				
Std. Dev.	0.21				R-Squared	0.9236
Mean	2.04				Adj R-Squared	0.8883
C.V. %	10.10				Pred R-Squared	0.7849
PRESS	1.55				Adeq Precision	17.565

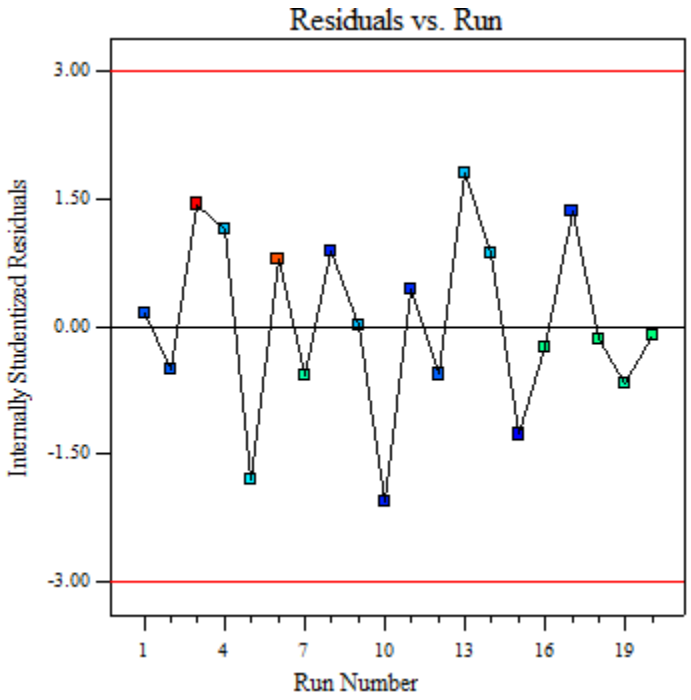

Fig. 4. Plot of residuals vs runs for surface roughness.

straight line. It denotes allotment of errors generally and also the significance of the models. Figure 4 demonstrates the residuals regarding experimental runs. This concludes the natural irregularity in the residuals and does not display any pattern with run order. The point is the absence of any clear pattern and the abnormal arrangement is shown in Fig. 5, which indicates that the recommended model is more than sufficient to establish the shape of surface roughness. Figure 5 shows the actual surface roughness versus the predicted surface roughness. As the predicted values come closer to the actual values, the points on the plot fall closer around the line. There is a strong correlation between the model's predictions and its actual

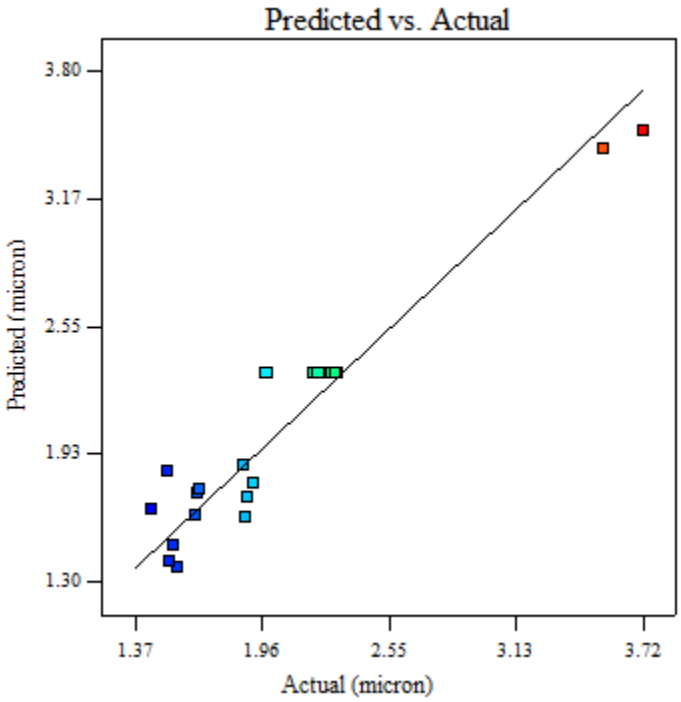

Fig. 5. Closeness of experimental value vs predicted value shown with reference to $Y = X$ line.

results. The p-values are all very small (< 0.0001) in the ANOVA table. This indicates that all three effects (cutting speed, feed and depth of cut) contribute significantly when predicting surface roughness.

The 3D response surface plots were made to examine the effects of each parameter on the R_a as illustrated in Fig. 6. A combination of lower cutting speed and lower feed which presents the better R_a is illustrated in Fig. 6(a). The inference is that the cutting speed value of 173.5 meter/minute and feed of 0.1 millimeter/revolution increases the R_a. Figure 6(b) interaction plots show a good R_a at a lower feed and intermediate depth of cut. In Figure 6(c), good R_a are provided by lower or higher cutting speeds and an intermediate depth of cut. These interaction plots demonstrate the mixture of higher cutting speed (245 meter/minute) along with lower feed (0.051 millimeter/revolution) and middle depth of cut (0.75 millimeter) which provides the lowest R_a when SG iron is machined with CBN insert. Similar examples of results have also been obtained in machining difficult materials with CBN by previous researchers [16, 17]. A high-quality surface finish could be achieved by maintaining the speed and depth of cut at a constant rate [18].

3.2. Surface Roughness of SG Irons with Coated WC Tool

Using the least square fitting model, the following second order equation for R_a with cutting parameters has been developed.

$$R_a = -8.03689E-003 + 0.046331 * v - 58.89972 * f - 0.98047 * d + 22.20886 * f * d - 1.23524E - 4 * v^2 + 274.89707 * f^2 \quad (2)$$

The ANOVA technique based on F and P-value helps verification of the adequacy of the model. It infers that the model is significant from the F-value of 39.07 shown in the ANOVA Table 5. There is only a 0.01% chance that a "Model F-value" of this large could occur due to noise. The values of "prop $> F$" less than 0.05 indicates the model terms are significant. In this case, v, f, d, fd, v^2, and f^2 are significant model terms. R^2 value is 0.9475 which is close to unity has proven the efficiency of the model. It exhibits the

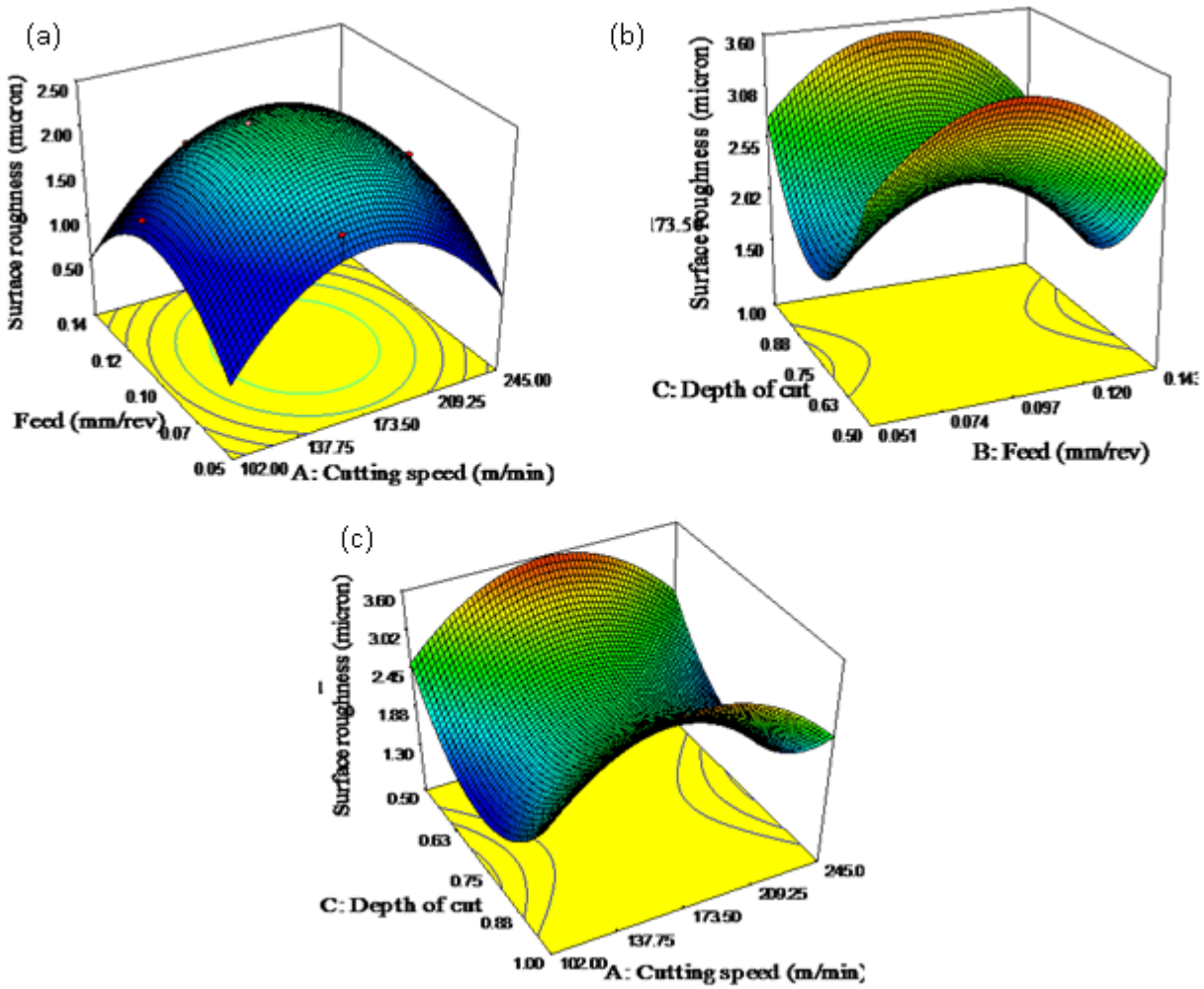

Fig. 6. (a) Effect of cutting speed & feed on surface roughness; (b) effect of feed & depth of cut on surface roughness; (c) effect of cutting speed & depth of cut on surface roughness.

existence of a high relationship between investigations and predicted values. In addition, the "Adjusted R^2" value (0.9232) is in close concurrence with the "Predicted R^2" value (0.8711) as desired. The non-inclusion of unnecessary terms is shown in this example. Signal to noise ratio is determined by "Adeq Precision". A ratio larger than four is attractive. From Table 5, Adeq Precision of 22.68 shows a satisfactory sign. Lower estimation of the coefficient of variation (C.V. = 7.73%) demonstrates enhanced exactness and reliability of the experimental trials.

The diagnostic details of this model have been carried out by using residuals versus results. These are presented in Figs. 7 to 9. The normal plot of residuals (Fig. 7) points out the appearance of residuals as a straight line which implies the significance of the models. The experimental runs with residuals are presented in Fig. 8. This implies the random nature of the residuals and does not exhibit any pattern with run order. Figure 9 establishes that there is no clear pattern and abnormal construction. This implies the adequacy of the proposed model to show the design of R_a. Figure 9 shows the actual surface roughness versus the predicted surface roughness. As the predicted values come closer to the actual values, the points on the plot fall closer around the line. There is a strong correlation between the model's predictions and its

Table 5. ANOVA results for surface roughness in turning SG iron with coated WC tool.

Source	Sum of Squares	Df	Mean Square	F Value	p-value Prob $> F$	Remarks
Model	5.76	6	0.96	39.07	< 0.0001	Significant
v-Cutting speed	0.62	1	0.62	25.04	0.0002	
f-Feed	2.60	1	2.60	105.89	< 0.0001	
d-Depth of cut	0.86	1	0.86	35.04	< 0.0001	
Fd	0.52	1	0.52	21.29	0.0005	
v2	1.12	1 7 1.12	45.78	< 0.0001		
f2	1.05	1	1.05	42.88	< 0.0001	
Residual	0.32	13	0.025			
Lack of Fit	0.28	8	0.035	4.55	0.0561	Not significant
Pure Error	0.039	5	7.720E-03			
Cor Total	6.08	19				
Std. Dev.	0.16				R-Squared	0.9475
Mean	2.03				Adj R-Squared	0.9232
C.V. %	7.73				Pred R-Squared	0.8711
PRESS	0.78				Adeq Precision	22.680

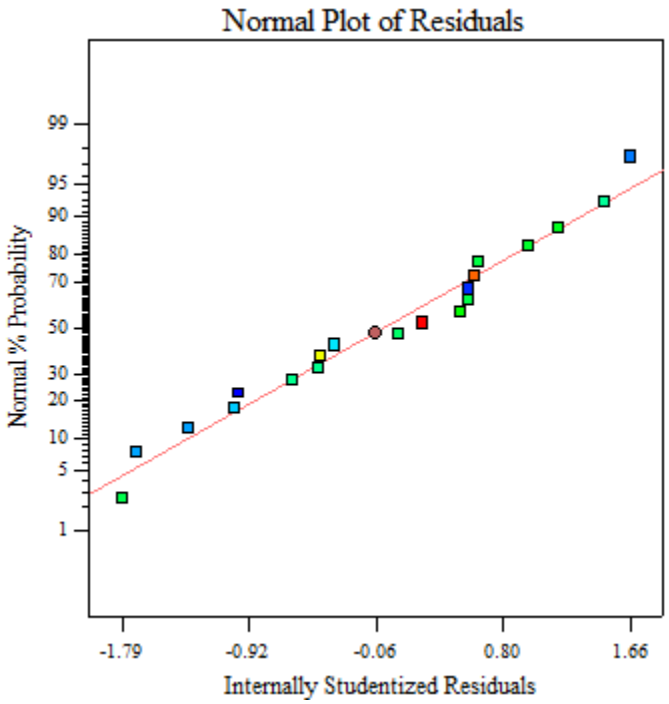

Fig. 7. Normal Probability plot of residuals for surface roughness.

actual results. The p-values are all very small (< 0.0001) in the ANOVA table. This indicates that all three effects (cutting speed, feed and depth of cut) contribute significantly when predicting surface roughness. It has been found that the % of error after comparing the actual and predicted values, the errors falls well within the permissible range ($\pm$ 10%). Therefore, the developed analytical models (Eq. 2) deem to be valid.

The 3D response surface plots were drawn for analysis of the influence of each parameter on the R_a as shown in Fig. 10. Figure 10(a) shows the interaction between cutting speed, feed versus R_a the increase in R_a as a cause of the increase in the feed and R_a being the minimum at lower speed are illustrated. The R_a

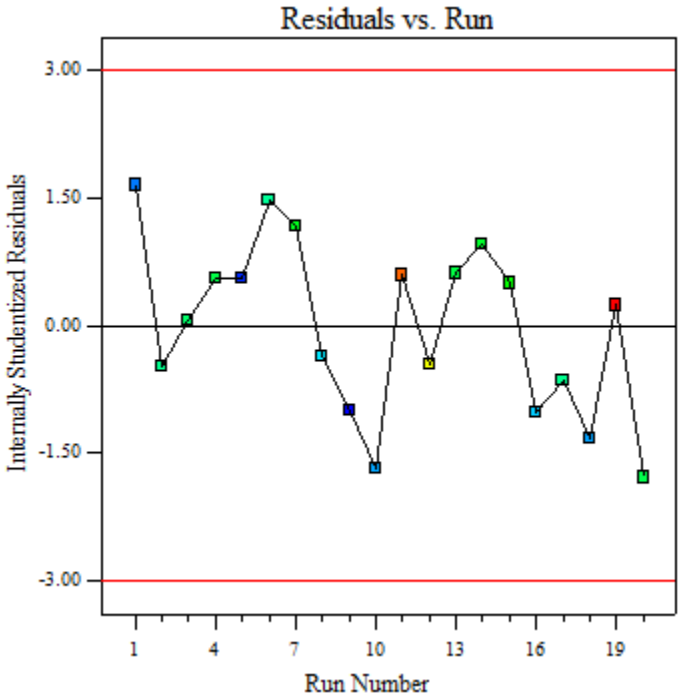

Fig. 8. Plot of residuals vs runs for surface roughness.

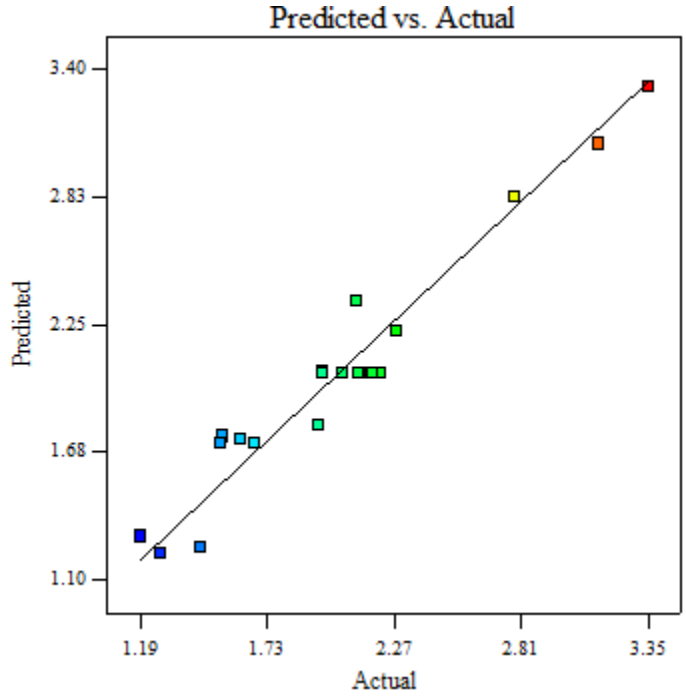

Fig. 9. Closeness of experimental value vs predicted value shown with reference to $Y = X$ line.

values of ductile iron material are higher when the cutting speed is increased from 102 meter/minute to 173.5 meter/minute. Thereafter its value reduces gradually. This is due to the formation of BUE at a lower speed at the tool tip at a low cutting speed. Improved surface finish is accomplished when the cutting temperature

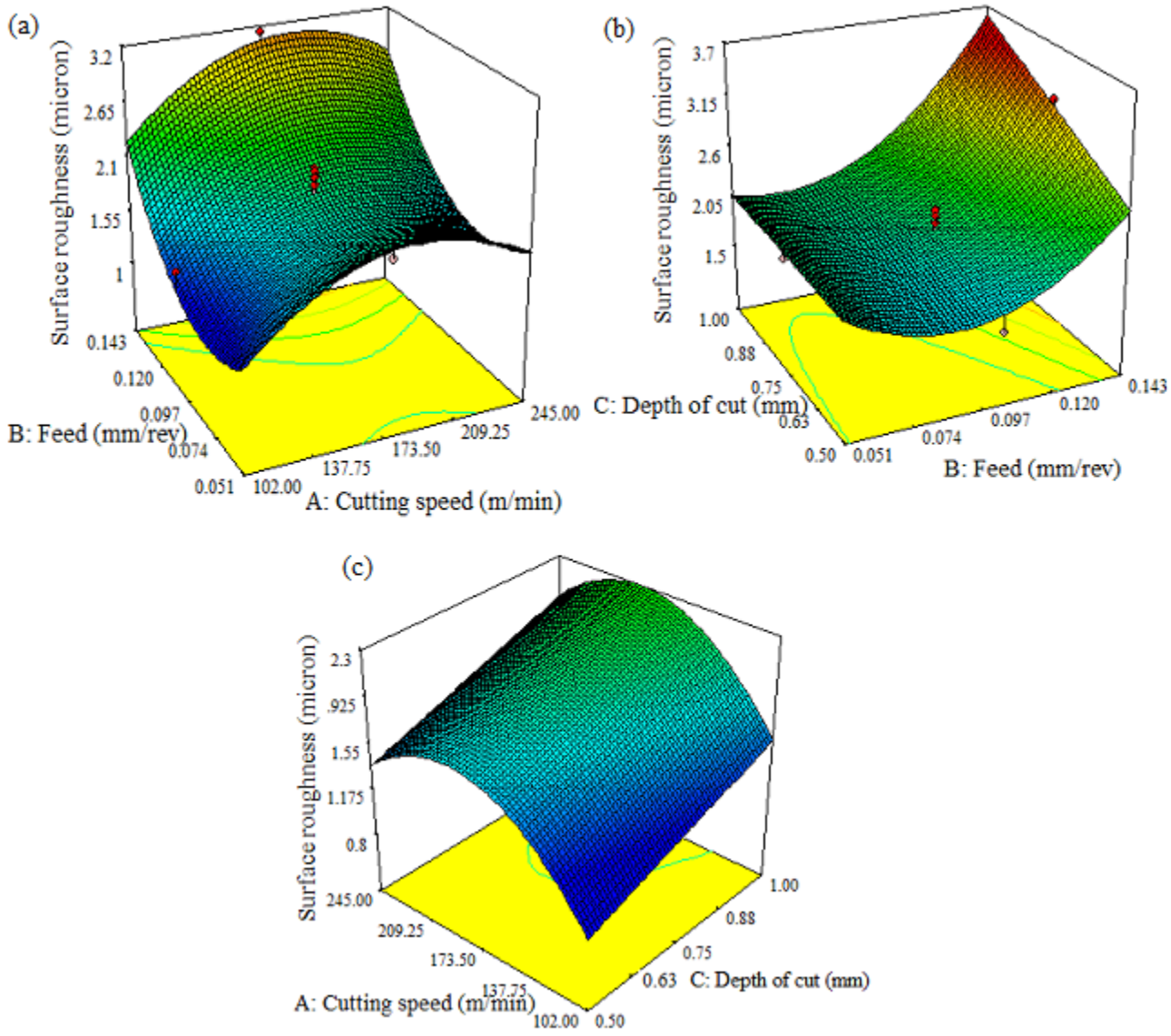

Fig. 10. (a) Effect of cutting speed & feed on surface roughness; (b) effect of feed & depth of cut on surface roughness; (c) effect of cutting speed & depth of cut on surface roughness.

raises and reduces build-up edge on the tip of the tool. The same observation was also covered by previous researchers [3, 19]. Coated tools past a certain speed of machining could be distributed to the incident of rubbing during turning results in the fall of R_a [20]. Figure 10(b) shows poor R_a being obtained at high feed and a total absence of any influence of depth of cut. Figure 10(c) demonstrates R_a being maximum when depth cut is increased and good surface finish is attained at a lower cutting speed. The changes in the feed show higher sensitivity in R_a compared to other parameters [21]. These interaction plots demonstrate the combination of lower cutting speed (102 meter/minute) along with a lower depth of cut and lower feed which offer the lowest R_a of SG iron with a coated WC tool. The multilayer coated cutting tool produces the best R_a at lower feed and higher speed [22].

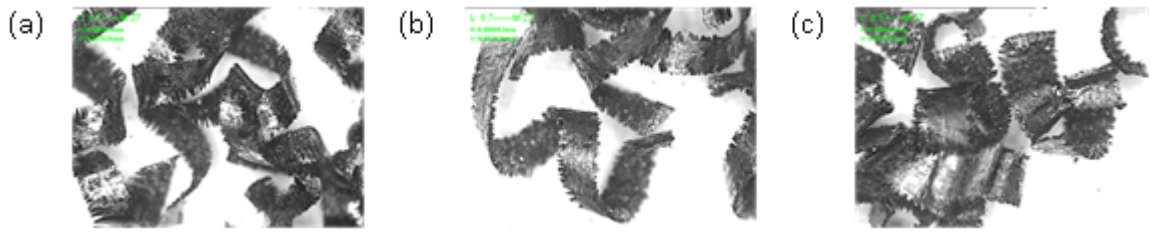

Fig. 11. Chip formation (50X) (a) semi continuous with curl chip; (b) ribbon type chip; (c) short segmented chip.

4. CHIP MORPHOLOGY

The variables influencing chip morphology are identified with the chemical composition of the material, microstructure, and material removal parameters [23]. Shear localized chip, discontinuous chip, segmental chip, and wavy chip are the other names for the arrangement of saw tooth chips, which results in hard alloys and hard steels by the use of the cutting systems [24]. This assortment of chips has been observed previously by many investigators [25, 26]. The chips obtained from this experimental study are shown in Fig. 11. In this work, all chips presented were segmented (discontinuous). Three different types of chips were observed: a semi-continuous with a twist, strip sort and short fragmented chip. Chip forms vary from tool material to tool material at different cutting speed. Chips of ductile iron materials turned into spiral rolled chip crumbs and were flat and smooth [27].

5. CONCLUSIONS

The main focus of this study has been the numerical modeling of R_a utilizing RSM, and analysis of chip morphology when machining spheroidal graphite iron (SG Iron) with a CBN and coated WC tool.

The following conclusions have been made on the basis of the results:

1. R_a tests show SG iron machining with CBN insert offering better R_a at the combination of higher cutting speeds, lower feeds, and depths of cut.

2. In the view of best R_a, the tool which is the coated WC tool is suited for lower cutting speeds, lower feeds, and lower depths of cut.

3. Subsequently, the feed is the most impacting parameter for both CBN and coated WC cutting tools for predictions on R_a contained by the limit of the factors taken up for investigation.

4. Segmented chips are shown in all cutting conditions. Chip forms are changed from one tool material to another at different cutting speeds.

REFERENCES

1. Grzesik, W., Kiszka, P., Kowalczyk, D., Zak, K. and Rech, J., "Investigation of the machining process of spheroidal cast iron using CBN tools", *Metabk*, Vol. 53, No. 1, pp. 33–36, 2014.
2. Graham, D., "Machining cast iron", *Manufacturing Engineering*, Vol. 136, No. 2, www.sme.org, 2006.
3. Sekar, U. and Hasirci, H., "Evaluation of machinability of austempered ductile irons in terms of cutting forces and surface quality", *Journal of Material Processing Technology*, Vol. 173, pp. 260–268, 2006.
4. Ductile iron data for designing Engineer, Ductile iron society (DIS), http://www.ductile.org, 2001.
5. Karsay, S.I., "Ductile iron I production", Quebec Iron and Titanium Corporation; Canada, 9, 71, 88,103-104,109,111 and 182, 1985.
6. Trent, E.M., *Metal Cutting*, Tanner Ltd., London, 1984.

7. *The Iron Casting Handbook*, Iron Casting Society Inc., 1981.
8. *Machining Data Handbook*, 3rd ed, Metcut Research associates Inc., Cincinnati, OH, 1980.
9. *Machining Ductile Irons*, International Nickel Co. Inc., New York, 2001.
10. Cakir, M.C., Bayram, A., Isik, Y. and Salar, B., "The effect of austempering temperature and time onto the machinability of austempered ductile iron", *Materials science and Engineering A*, Vol. 407, pp. 147–153, 2005.
11. Diniz, A.E., Marcondes, F.C. and Coppini, N.L., *Technologia da Usinagem dos Materials*, 5th ed., Artliber Editora, Sao Paulo, 2006.
12. Grzesik, W., Rech, J., Zak, K. and Claudin, C., "Machining performance of pearlitic-ferritic nodular cast iron with coated carbide and silicon nitride ceramic tools", *International Journal of Machine Tools & Manufacture*, Vol. 49, pp. 125–133, 2009.
13. Santhanam, A.T., "Carbide's for metal cutting", in *Kennametal Comprehensive Application Engineering Guide*, Kennametal University, Latrobe, PA, Vol. 1, pp. 3–6, 2005.
14. Srivastava, A.K. and Finn, M.E., "Machining cast iron components", Modern casting, AFS, IL, USA. http://www.afsinc.org/multimedia/contentMC.cfm?ItemNumber=11371
15. Montgomery, D.C., *Design and Analysis of Experiments*, John Wiley & Sons, New York, 2001.
16. Chavoshi, S.Z. and Tajdari, M., "Surface roughness modelling in hard turning operation of AISI 4140 using CBN cutting tool", *Int. J. Mater. Form.*, Vol. 3, No. 4, pp. 233–239, 2010.
17. Auoici, H., "Analysis of surface roughness and cutting force component in hard turning with CBN tool: Prediction model and cutting condition optimization", *Measurement*, Vol. 45, No. 3, pp. 344–353, 2012.
18. Datt, J. and Batra, U., "Influence of composition and austempering temperature on machinability of austempered ductile iron", *International Journal of Chemical, Nuclear, Materials and Metallurgical Engineering*, Vol. 7, No. 2, 2013.
19. Aslantas, K. and Ucun, I., "The performance of ceramic and cermet cutting tools for machining of austempered ductile iron", *Int. J. Adv. Manuf. Technol.*, Vol. 41, pp. 642–650, 2009.
20. Shanmugam, S. and Krishnamurthy, R., "Machinability study on pearlitic spheroidal graphite cast iron", *International Journal of Production Research*, Vol. 30, No. 1, pp. 189–197, 2007.
21. Kacal, A. and Gulesin, M., "Determination of optimal cutting conditions in finish turning of austempered ductile iron using taguchi design method", *Journal of Scientific & Industrial Research*, Vol. 70, pp. 278–283, 2011.
22. Kribes, N., Hessainia, Z. and Yallese, M.A., "Optimization of machining parameters in hard turning by desirability function analysis using Response Surface Methodology", in *Proceedings of the Sixth Conference on Design and Modeling of Mechanical Systems*, Hammamet, Tunisia, 2015.
23. Dubensky, W.J. and Rundman, K.B., "An electron microscope study of carbide formation in austempered ductile iron", *Trans. Am. Foundry Soc.*, Vol. 64, No. 85, pp. 389–394, 1985.
24. Komanduri, R. and Brown, R.H., "The mechanics of chip segmentation in machining", *ASME J. Eng. Ind.*, Vol. 103, No. 1, pp. 33–51, 1981.
25. Pashby, I.R., Wallbank, J. and Boud, F., "Ceramic tool wear when machining austempered ductile iron", *Wear*, Vol. 162–164, pp. 22–33, 1993.
26. Vasconcelos de Carvalho, M., et al., "An analysis of the machinability of ASTM grades 2 and 3 austempered ductile iron", *Journal of Materials Processing Technology*, Vol. 213, pp. 560–573, 2013.
27. Guo, X. and Wan, D., "An experimental study on machinability of austempered ductile iron during dry turning by ceramic cutting tools", in *Proceedings of the ASME 2012 International Design Engineering Technical Conferences & Computer and Information in Engineering Conference*, Chicago, IL, USA, 2012.